View metadata, citation and similar papers at core.ac.uk
brought to you by CORE
provided by Sheffield Hallam University Research Archive

Breakup Branches of Borromean Beryllium-9

R. Smith[1,a)], M. Freer[1], C. Wheldon[1], N. Curtis[1], S. Almaraz-Calderon[2], A. Aprahamian[2], N. I. Ashwood[1], M. Barr[1], B. Bucher[2], P. Copp[3], M. Couder[2], X. Fang[2], G. Goldring[4], F. Jung[2], Tz. Kokalova[1], S. R. Lesher[3], W. Lu[2], J. D. Malcolm[1], A. Roberts[2], W. P. Tan[2] and V. A. Ziman[1]

[1]*School of Physics and Astronomy, University of Birmingham, Edgbaston, Birmingham, B15 2TT, UK.*
[2]*Institute for Structure and Nuclear Astrophysics, Department of Physics, University of Notre Dame, Notre Dame, IN 46556, USA.*
[3]*Department of Physics, University of Wisconsin - La Crosse, La Crosse, WI 54601, USA.*
[4]*Department of Particle Physics, Weizmann Institute, 76100 Rehovot, Israel.*

[a)]r.smith.3@pgr.bham.ac.uk

Abstract. The breakup reaction ^{9}Be(^{4}He, 3α)*n* was measured using an array of four double-sided silicon strip detectors at beam energies of 22 and 26 MeV. Excited states in ^{9}Be up to 12 MeV were populated and reconstructed through the measurement of the charged reaction products. It is proposed that limits on the spins and parities of the states can be derived from the way that they decay. Various breakup paths for excited states in ^{9}Be have been explored including the ^{8}Be$_{g.s.}$ + *n*, ^{8}Be$_{2^+}$ + *n* and ^{5}He$_{g.s.}$ + ^{4}He channels. By imposing the condition that the breakup proceeded via the ^{8}Be ground state, clean excitation spectra for ^{9}Be were reconstructed. The remaining two breakup channels were found to possess strongly-overlapping kinematic signatures and more sophisticated methods (referenced) are required to completely disentangle these other possibilities. Emphasis is placed on the development of the experimental analysis and the usefulness of Monte-Carlo simulations for this purpose.

INTRODUCTION

Beryllium-9 can be thought to consist of two α particles along with a neutron that resides in molecular orbits about the α cores [1]. The nucleus has just one bound state - the ground state - and is Borromean as no pairings of the three cluster constituents (either ^{8}Be or ^{5}He) form a bound system. Therefore, a reaction that populates an excited state in ^{9}Be inevitably results in a breakup into these cluster components through a number of possible intermediate states. This three-particle molecular picture of ^{9}Be is supported by state-of-the-art calculations such as the Antisymmetrized Molecular Dynamics (AMD) and No-Core Shell Model (NCSM) approaches that report the *ab initio* emergence of this structure [2, 3]. It is thought that the low-lying excitation spectrum of ^{9}Be can be grouped into rotational bands corresponding to the collective rotation of different intrinsic molecular configurations.

However, ^{9}Be still remains an exceptionally difficult nucleus to study experimentally because the excited states typically exist as broad resonances above the particle decay threshold. Due to the propensity for these states to decay through particle emission, gamma decay data, traditionally so important for the conformation of rotation, are scarce. Therefore, the signatures of rotational structures are typically based on the identification of patterns in the excitation energies and the spins of excited levels. Even so, a significant number of documented levels above 3 MeV have tentative spin an parity assignments, leading to persistent and significant ambiguities in the experimental spectrum. Therefore, the nature of the ^{9}Be spectrum has been subject to decades of experimental conjecture.

This proceedings contribution presents an ongoing, high-statistics experimental study of the ^{9}Be excitation spectrum using the method of charged particle spectroscopy. States up to 12 MeV in ^{9}Be were populated through the inelastic scattering of ^{4}He nuclei and analysis methods have been developed in order to determine the breakup yields for states to decay through a number of key channels; the eventual aim being to place limits their spins and parities.

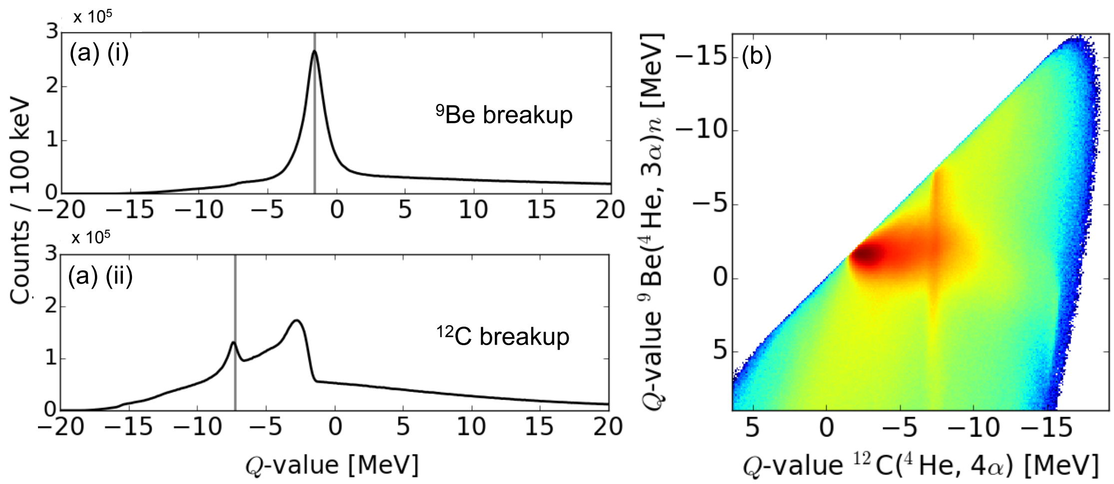

FIGURE 1. (a) Histograms of the calculated Q-values (26 MeV beam data only†) assuming (i) an interaction with ^{9}Be in the target and (ii) an interaction with ^{12}C in the target. The ^{9}Be Q-value peak has a resolution (FWHM) of around 1.9 MeV and the ^{12}C peak has a resolution of 0.9 MeV. The vertical lines mark the known reaction Q-values of -1.57 and -7.28 MeV. (b) (color online) The same data visualised on a 2D plot. † Similar plots were generated using the 22 MeV beam energy data.

EXPERIMENTAL DETAILS

The experimental data were acquired using a ^{4}He beam ($Q = 2^+$), from the Notre Dame tandem Van de Graaff accelerator, incident on a ^{9}Be target of thickness 1000 μg cm^{-2} . Two separate runs were performed at beam energies of 22 and 26 MeV. The breakup reaction of ^{9}Be(^{4}He, 3α)n was measured using an array of four in-plane 500-μm-thick, *Micron* double-sided silicon strip detectors (DSSSDs), each possessing a total active surface area of 5×5 cm^2. Each was aligned with the centre of the detector plane perpendicular to the target position and at distances ranging between 6 and 10 cm from this point. The detectors were placed at centre angles $-69°$, $-30°$, 33° and 71°, with respect to the beam direction, providing a continuous angular coverage from 16° to 90°. The segmented geometry of the detectors allowed both the energy and the position of a detection to be measured.

The detectors were calibrated using a ^{148}Gd and ^{241}Am source corresponding to α particle decay energies of 3.183 and 5.486 MeV respectively. The detectors and processing electronics resulted in a typical energy resolution of around 100 keV (full width at half maximum, FWHM) across each detector. Measuring elastic scattering from ^{197}Au and ^{12}C targets allowed the verification of the distances, angles and energy calibrations of each detector. The processing electronics demanded a detection multiplicity condition of three coincident hits to record an event.

ANALYSIS

Since the detectors had no explicit particle identification, selection of the reaction-channel was achieved through a reconstruction of the reaction kinematics. The vector momenta of each detected particle were calculated, presuming each to be a final-state ^{4}He nucleus. Assuming that the incident ^{4}He interacts with a ^{9}Be nucleus in the target via ^{9}Be(^{4}He, 3α)n, by detecting the energies and angles of the scattered ^{4}He beam particle along with the two ^{4}He resulting from the breakup of ^{9}Be (detection multiplicity condition of 3), it is possible to reconstruct the properties of the undetected final-state neutron using momentum conservation. The reaction Q-value for each event was then calculated as the difference between the sum of the energies in the final-state and the beam energy.

Similarly, assuming that the incident ^{4}He interacts with a ^{12}C contaminant nucleus in the target through ^{12}C(^{4}He, 4α), a reaction Q-value for this process was calculated for each event. In order to select the ^{9}Be channel, the Q-value histograms in Fig. 1 were constructed. The reaction of interest was then selected by placing a cut centred on the peak in the ^{9}Be Q-value spectrum. Data within the narrow ^{12}C peak were discarded. The remaining background consists of random coincidences along with the breakup of ^{16}O in the target.

Analysing the relative energies between pairs of detected particles provided a way to restrict the possible final-

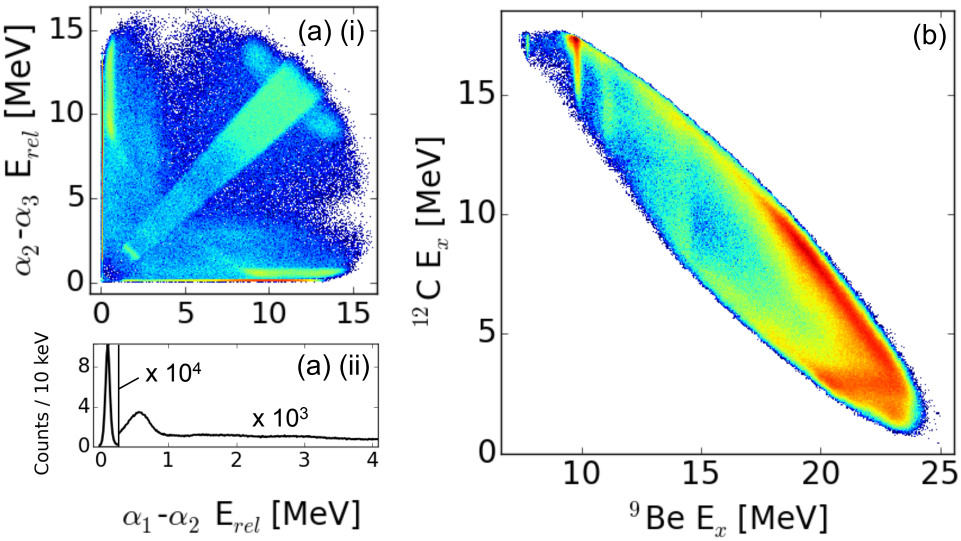

FIGURE 2. (color online) (26 MeV beam data only†) (a) (i) α-α relative energies for particular combinations of final state particles. Narrow vertical and horizontal bands at 92 keV correspond to decays via the ^{8}Be ground state. Broader bands can be identified near to 3 MeV, corresponding to the $^8\mathrm{Be}_2^+$ breakup channel. The diagonal bands occur when a α_1 and α_3 originate from a ^{8}Be intermediate state. (ii) 1D projection of the plot with a magnified horizontal energy scale. The bump at 0.6 MeV has been shown to correspond to decays from the ^{9}Be 5/2$^-$ state to the tail of the ^{8}Be 2$^+$ level [4]. (b) Dalitz plot of the 26 MeV beam data. States associated with ^{12}C breakup appear as vertical bands and ^{9}Be breakups form the broad horizontal bands. Neutron transfer events form the diagonal locus. † Similar plots were generated using the 22 MeV beam energy data.

state interactions. In particular, the $^8\mathrm{Be}_{g.s.}$ + n, $^8\mathrm{Be}_{2^+}$ + n and $^5\mathrm{He}_{g.s.}$ + ^{4}He breakup channels of ^{9}Be were considered. Of the three detected ^{4}He, it is possible that two of these arose from the breakup of an intermediate ^{8}Be state, should ^{9}Be have decayed through neutron emission. The final-state ^{4}He were randomly labelled α_1, α_2 and α_3, then the relative energies between possible pairs were calculated for each event. These are illustrated in Fig. 2 a). Breakups through the $^8\mathrm{Be}_{g.s.}$ channel were selected with < 1% background by placing cuts on the narrow peaks at 92 keV. The excitation of ^{9}Be could then be calculated.

With this breakup criterium in place, there still remain a number of reaction channels that can account for the 3α + n final state. To disentangle the origins of the detected particles, the Dalitz plot shown in Fig. 2 b) was constructed. Both ^{9}Be(^{4}He,n)^{12}C and ^{9}Be(^{4}He,^{5}He)^{8}Be reactions are identified on the plot and were omitted from further analysis. Consequently, clean excitation spectra for ^{9}Be, corresponding to the $^8\mathrm{Be}_{g.s.}$ + n channel, have been calculated for each beam energy. Q-value cuts placed either side of the peak in Fig. 1 a) i) were used to gauge a background for each spectrum.

To determine the true breakup yields, Monte-Carlo simulations of the reaction were performed, using the RES8 code, to correct the spectra for the efficiency of the detection system [5]. Further Monte-Carlo simulations demonstrated that the experimental resolution varied between around 600-700 keV across the whole spectrum. Detailed fits to the spectra were performed and allowed the energies, widths, and amplitudes of the known levels in ^{9}Be to be extracted. The excitation spectra and fit results are not discussed here.

To place limits on the spins and parities of the ^{9}Be levels populated in the experiment, breakups through other channels must be considered. When a nucleus decays by particle emission, the breakup rate is predominantly determined by the penetrability through the Coulomb and centrifugal barriers. Therefore, by accurately measuring the frequency with which a state in ^{9}Be decays through two or more channels of different angular momentum (for example $^8\mathrm{Be}_{g.s.}$ (0$^+$) + n and $^8\mathrm{Be}_{2^+}$ + n), information regarding the centrifugal barrier for the decay, and therefore the angular momentum of the decaying state, can be extracted.

Breakups through both the $^8\mathrm{Be}_{2^+}$ + n and $^5\mathrm{He}_{g.s.}$ + ^{4}He channels can be selected by demanding that the α-α relative energy lies above the $^8\mathrm{Be}_{g.s.}$ peak. Although Fig. 2 a) clearly shows breakups through $^8\mathrm{Be}_{2^+}$ (broad horizontal and vertical bands at $\approx$ 3 MeV), Monte-Carlo simulations demonstrate that $^5\mathrm{He}_{g.s.}$ breakups manifest as an intractable background in this region. An alternative analysis considers the relative energies between the neutron and ^{4}He in the

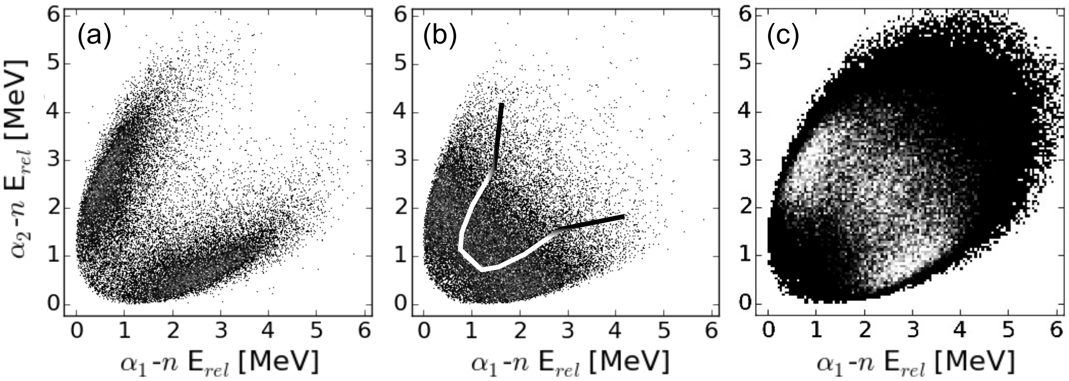

FIGURE 3. (26 MeV beam energy only†) Plots of α-n relative energies for a) Monte-Carlo simulations of the $^{5}He_{g.s.}$ breakup of a 6 MeV level in ^{9}Be, b) simulations of the $^{8}Be_{2^+}$ breakup of a 6 MeV level in ^{9}Be, and c) Plot of the experimental data with a $5.5 \leq E_x \leq 6.5$ MeV excitation energy cut. Plot b) shows the relative energy cut that can be used to select $^{8}Be_{2^+}$ breakups with minimal contributions from the $^{5}He_{g.s.}$ channel. † Similar plots were generated using the 22 MeV beam energy data.

final state [6]. The ^{4}He that result from the breakup are randomly labelled α_1 and α_2. Plots of the relative energies α_1-n vs α_2-n (simulated $^{5}He_{g.s.}$ breakups) are shown in Fig. 3 a). Since ^{5}He is unbound by 735 keV, the presence of $^{5}He_{g.s.}$ breakups are indicated by event concentrations around 735 keV on one axis and around a relatively higher energy on the other. Comparing this with the signature for $^{8}Be_{2^+}$ breakups in Fig. 3 b) demonstrates that there is a region (marked), which is only significantly occupied by $^{8}Be_{2^+}$ breakup events. These can be selected by applying a software cut in the marked region. Figure 3 c) depicts the experimental data in this excitation region and shows the bands of high intensity corresponding to $^{5}He_{g.s.}$ breakups. The software cut is only effective for high excitations in ^{9}Be. The allowed phase space in the α-n plots decreases with the ^{9}Be excitation, so, at low excitations, there is a large overlap between the two breakup channels. More sophisticated analyses are required in order to separate them [4].

OUTLOOK

The breakup branches of the borromean ^{9}Be nucleus can be disentangled through the analyses presented in this paper. Beryllium-9 excitation spectra corresponding to breakups through the $^{8}Be_{g.s.}$ were cleanly reconstructed and fits to these spectra form the discussion for a follow-up paper currently under preparation. Excitation spectra for the $^{8}Be_{2^+}$ breakup channel can be cleanly reconstructed, but only for $E_x \gtrsim 4$ MeV. Overlapping kinematic signatures at low excitation mean that the $^{8}Be_{2^+}$ and $^{5}He_{g.s.}$ channels cannot be separated, leading to challenges when efficiency-correcting the experimental spectra, which is necessary to quantify the breakup yields.

ACKNOWLEDGMENTS

R. Smith would like to thank the Notre Dame Tandem operators for their work over the course of this experiment.

REFERENCES

[1] W. von Oertzen, Z. Phys. A. Hadron Nucl **354**, 37–43 (1996).
[2] Y. Kanada-En'yo and H. Horiuchi, Prog. Theor. Phys. Supplement **142**, 205–263 (2001).
[3] P. Maris and J. P. Vary, Int. J. Mod. Phys. E. **22**, p. 1330016 (2013).
[4] P. Papka, T. A. D. Brown, B. R. Fulton, D. L. Watson, S. P. Fox, D. Groombridge, M. Freer, N. M. Clarke, N. I. Ashwood, N. Curtis, V. Ziman, P. McEwan, S. Ahmed, W. N. Catford, D. Mahboub, C. N. Timis, T. D. Baldwin, and D. C. Weisser, Phys. Rev. C **75**, p. 045803 (2007).
[5] N. Curtis, Resolution 8 (RES8) Monte-Carlo Code, Unpublished, Accessed: 2014.
[6] T. A. D. Brown, P. Papka, B. R. Fulton, D. L. Watson, S. P. Fox, D. Groombridge, M. Freer, N. M. Clarke, N. I. Ashwood, N. Curtis, and *et al.*, Phys. Rev. C **76**, p. 054605 (2007).